Immunity
Article

Toll-like Receptor 4 Signaling by Follicular Dendritic Cells Is Pivotal for Germinal Center Onset and Affinity Maturation

Alexandre Garin,[1,6,7] Michael Meyer-Hermann,[2,3,6] Mathias Contie,[1] Marc Thilo Figge,[3] Vanessa Buatois,[1] Matthias Gunzer,[4] Kai-Michael Toellner,[5] Greg Elson,[1] and Marie H. Kosco-Vilbois[1,*]
[1]NovImmune SA, 14 chemin des Aulx, 1228 Plan les Ouates, Switzerland
[2]Department Systems Immunology, Helmholtz Centre for Infection Research (HZI), Inhoffenstr. 7, D-38124 Braunschweig, Germany
[3]Frankfurt Institute for Advanced Studies (FIAS), Ruth-Moufang-Str. 1, D-60438 Frankfurt am Main, Germany
[4]Institute for Molecular and Clinical Immunology, Otto-von-Guericke-University, Leipziger Str. 44, D-39120 Magdeburg, Germany
[5]MRC Centre for Immune Regulation, College of Medicine and Dental Sciences, University of Birmingham, Edgbaston, B15 2TT Birmingham, UK
[6]These authors contributed equally to this work
[7]Present address: Merck Serono S.A., 9 Chemin des Mines, 1202 Geneva, Switzerland
*Correspondence: mkosco-vilbois@novimmune.com
DOI 10.1016/j.immuni.2010.07.005

SUMMARY

Germinal centers (GCs) are specialized microenvironments where antigen-activated B cells undergo proliferation, immunoglobulin (Ig) class switch recombination, somatic hypermutation (SHM), and affinity maturation. Within GCs, follicular dendritic cells (FDCs) are key players in driving these events via direct interaction with GC B cells. Here, we provide in vivo evidence that FDCs express and upregulate Toll-like-receptor (TLR) 4 in situ during germinal center reactions, confirm that their maturation is driven by TLR4, and associate the role of FDC-expressed TLR4 with quantitative and qualitative affects of GC biology. In iterative cycles of predictions by in silico modeling subsequently verified by in vivo experiments, we demonstrated that TLR4 signaling modulates FDC activation, strongly impacting SHM and generation of Ig class-switched high-affinity plasma and memory B cells. Thus, our data place TLR4 in the heart of adaptive humoral immunity, providing further insight into mechanisms driving GCs arising in both health and disease.

INTRODUCTION

The central function of B cells during innate or adaptive immune responses to infections is the production of antimicrobial Ig. The initiation of the innate response is through so-called danger signals, provided by activation of host pattern recognition receptors (PRR) via pathogen-associated molecular footprints (Akira et al., 2001). The most commonly used PRR in mammals are Toll-like receptors (TLR) that sustain innate immune responses by promoting secretion of proinflammatory cytokines (Akira et al., 2006). TLRs are also involved in adaptive immunity, promoting, for example, the maturation of dendritic cells (DCs) (Lee and Iwasaki, 2007). Although the existence of a direct axis between TLRs and B cells to promote humoral responses, independently of TLR4 function on DCs and T cells, is contentious (Pasare and Medzhitov, 2005; Nemazee et al., 2006; Meyer-Bahlburg et al., 2007), TLR signaling has been reported to promote auto-Ab production (Marshak-Rothstein, 2006).

The cellular expression of TLRs is broad, including leukocytes (Banerjee and Gerondakis, 2007) and stromal, endothelial, or epithelial cells (Gribar et al., 2008; Iwamura and Nakayama, 2008). Recently, TLR4 expression has also been observed on FDCs (El Shikh et al., 2007), a radio-resistant cell type located in primary follicles and the light zone of GCs. However, TLR4 function on FDC has remained elusive. FDCs play a crucial role in the preventing GC B cell apoptosis (Kosco et al., 1992; Lindhout et al., 1993), promoting high-affinity Ig secretion (Aydar et al., 2005) and enhancing signals leading to SHM (Wu et al., 2008). FDCs activated in vitro with the TLR4 ligand lipopolysaccharide (LPS) upregulate adhesion molecules and provoke higher antigen (Ag)-specific Ig production when cocultured with B cells (El Shikh et al., 2007). Understanding how the sensors of innate immunity, such as TLR4 on FDCs, contribute to healthy humoral responses will provide insights into how aberrant GCs are formed and maintained during chronic diseases.

We report that endogenous TLR4 ligands are present within GCs and thus provide a self-potentiating source of host-derived receptor agonism. Furthermore, we explore the expression of TLR4 by FDCs and its function during the GC reaction. To narrow potential hypotheses to be tested in wet experiments, we applied in silico simulations of the GC reaction, based on a recently published mathematical model (Figge et al., 2008; Meyer-Hermann et al., 2009). The in silico experiments identified critical time points and experimental conditions to test in vivo. These experiments, conducted with both genetic as well as pharmaceutical approaches to abolish TLR4 function in FDCs, elucidated the kinetics of FDC-expressed TLR4 and mechanistically a TLR4 dependence for the downstream production of essential growth and differentiation factors. Loss of TLR4 signaling in FDCs resulted in a deficiency in the size and number of GC microenvironments, a paucity in mutational events in B cell

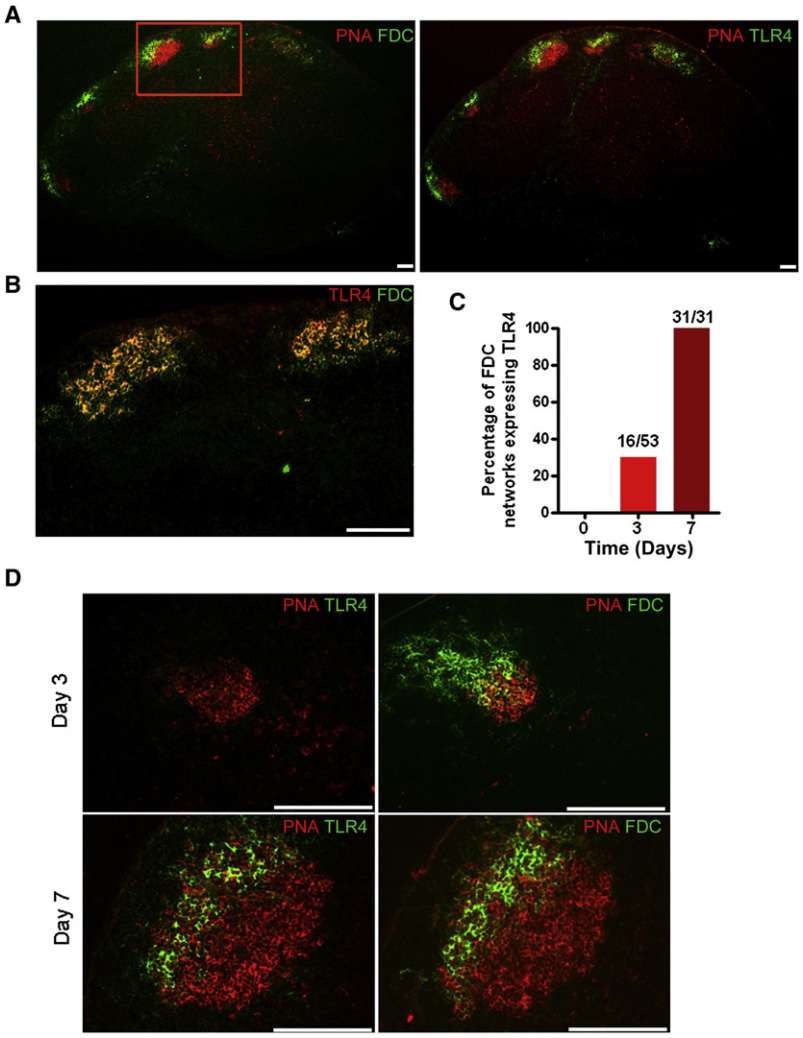

Figure 1. TLR4 Is Expressed on FDCs within the GC and Is Upregulated as FDCs Mature

(A) Balb/c mice (n = 10) were immunized with OVA plus LPS and 7 days later sections were prepared from LNs and colabeled with PNA and either the anti-TLR4 (5E3) or FDC-M1. Left and right panels represent consecutive tissue sections.

(B) Higher magnification of area boxed in (A, left) on a consecutive tissue section demonstrating colabeling of TLR4 expression (5E3) on FDC networks (FDC-M2).

(C) Quantitative analysis of at least 20 sections per LN per time point capturing the percent of FDC networks that were TLR4$^+$; values above columns represent the number of TLR4$^+$ networks observed within the total number of FDC-M2$^+$ networks evaluated per time point.

(D) Sections of LNs at 3 or 7 days postimmunization with OVA and LPS (n = 6 mice/time point). Consecutive sections were incubated with PNA and either anti-TLR4 mAb (left) or FDC-M2 (right). The day 3 and 7 photomicrographs included here are used to illustrate GC without and with TLR4-expressing FDC networks, respectively. The white bar in a photomicrograph represents its relative scale within the figure.

See also Figure S1.

receptor maturation, and a decrease in Ag-specific high-affinity Ig titers. Taken together, weaving in vivo and in silico results demonstrate a central role for TLR4 in the generation of optimal GC development and humoral responses.

RESULTS

FDCs Express TLR4

TLR4 expression during the GC reaction was assessed by analysis of lymph nodes (LNs) obtained from immunized mice. Seven days after immunization, the FDC network was identified (Figure 1A, left, green labeling) in PNA$^+$ GCs (Figure 1A, red labeling). In the consecutive section, TLR4 expression (Figure 1A, right, green labeling) was observed as a reticular pattern of labeling, markedly restricted to the anatomical compartment constituting the light zone of the GCs. Colabeling (Figure 1B) with TLR4 and FDC mAbs demonstrated that TLR4 expression was limited to the FDC network (yellow labeling) although not all FDCs were positive (green labeling). Corroborating the histological observations, TLR4 mRNA was present in purified FDC (data not shown), in contrast to GC B cells that showed no TLR4 labeling by histology (Figures 1B and 1D) nor detectable mRNA (data not shown). These in situ results demonstrate that FDC express TLR4 in vivo.

TLR4 Expression Is Upregulated during FDC Maturation

To investigate the kinetics of TLR4 expression on FDC during GC development, mice were immunized with OVA plus LPS and the draining LNs harvested prior to, as well as 3 and 7 days after, the immunization. Before immunization, no TLR4 labeling was observed on any FDC network (Figure 1C). By day 3 postimmunization, only 16 of the 53 FDC networks colabeled for TLR4 (Figures 1C and 1D illustrating a nonlabeled example), which was then upregulated within all networks by day 7 (Figures 1C and 1D). Similar results were obtained with alum, a non-TLR4 agonist, as adjuvant instead of LPS (data not shown), suggesting that exogenous TLR4 ligands are not required to upregulate TLR4 expression on FDCs. The kinetics of TLR4 expression by FDCs paralleled that of the FDC maturation markers, ICAM-1 (Figure S1A available online) and FcγRII and FcγRIII (Figure S1B), indicating that TLR4 expression is associated with FDC maturation. These results reveal that FDCs upregulate TLR4 expression during maturation.

Endogenous TLR4 Ligands Are Present within the GC

Because an upregulation of TLR4 on FDCs was observed, we hypothesized that an endogenous source of TLR4 ligands may exist in GCs. Sources of endogenous TLR4 agonists are the consequences of apoptosis, including oxidized phospholipids (OxPl) (Chang et al., 1999; Miller et al., 2003; Imai et al., 2008). Many GC B cells undergo apoptosis and are scavenged by tingible body macrophages (TBM), which are in close proximity to

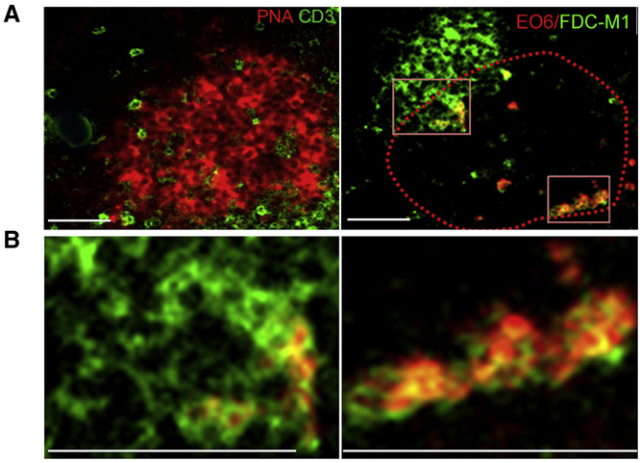

Figure 2. The Endogenous TLR4 Ligand OxPl Is Present within the GC

Balb/c mice (n = 6) were immunized with OVA plus LPS, and 9 days later, sections were prepared from LNs and labeled with combinations of PNA and an anti-CD3, or FDC-M1 and EO6 (specific for OxPl).

(A) The PNA^+ area (red) and anti-CD3 labeling (green) in the left panel permits orientation of the LN sections and identification of a PNA^+ GC. In the consecutive tissue section (right), the dotted area outlines the PNA^+ zone with the FDC network (green) oriented at the opposite pole of the $CD3^+$ T cell zone and morphologically identifiable TBM associated with endogenous TLR4 ligands (orange and yellow).

(B) Higher magnifications of the two areas within the squares of Figure 1A, depicting $OxPl^+$ (red) apoptotic bodies within the FDC network (left) and being engulfed by FDC-$M1^+$ TBM (right), producing an overlay of yellow and orange images. The white bar in a photomicrograph represents its relative scale within the figure.

FDCs. Therefore, host-derived TLR4 ligands may be generated within the GC and have access to the FDC network.

To test this hypothesis, draining LNs sections (9 days postimmunization) were consecutively colabeled with (1) PNA and anti-CD3 to identify the border of the GC dark zone (Figure 2A, left) or (2) FDC-M1 (labels both FDCs and TBMs) and EO6 (labels OxPl) (Chang et al., 1999). OxPls were detected within GCs, and FDC networks (yellow labeling, Figure 2A, right) could be observed within the GC (PNA-positive area in Figure 2A, left, used to indicate, by dotted line, the GC area in Figure 2A, right). At higher magnifications (Figure 2B), the labeling for OxPl was intimately associated with the FDC network (Figure 2B, left) as well as distal to the network, i.e., along the perimeter of the GC's dark zone (Figure 2B, right). Examining numerous sections provided consistent evidence that both TLR4 (on FDCs) and TLR4 ligands (OxPl in the GC) appeared in concert during the GC response. Taken together these results indicate that endogenous sources of TLR4 ligands exist and are available to activate FDC maturation during GC reactions.

Loss of TLR4 Function on FDCs Results in Altered Maturation and Impaired GC Development

In order to evaluate the biological consequence of TLR4 signaling by FDCs on GC development, parallel experimental approaches were applied. The first utilized was the blocking TLR4 mAb, 5E3. The TLR4 mAb was injected 3 days after immunization of mice. The absence of interference with DC maturation and T cell priming at this time point was confirmed by comparing expression of the maturation markers CD80 and MHC class II on DCs which were unaffected by anti-TLR4 treatment (data not shown).

The second approach involved generating mouse chimeras in which TLR4 was nonfunctional on FDCs. The C3H/HeJ strain, which carries a nonfunctional *Tlr4* gene (Poltorak et al., 1998), was used as the recipient of bone marrow (BM) from C3H/HeN mice (i.e., WT, TLR4 sufficient). These chimeric animals were compared to lethally irradiated C3H/HeN (WT) mice reconstituted with C3H/HeN (WT) BM. The radioresistant property of FDCs (Humphrey et al., 1984; Phipps et al., 1981) allowed the distinction of those effects mediated by TLR4 expression on hematopoietic cells versus host-maintained FDCs. No TLR4 expression was observed in GCs when the C3H/HeJ strain was used as host.

We first focused on evaluating the interdependence of TLR4, ICAM-1, and FcγRII and FcγRIII upregulation of FDCs. After immunization, ICAM-1 expression was enhanced on FDCs as expected (Figure 3A). In contrast, in anti-TLR4-treated mice, FDCs failed to upregulate ICAM-1 expression (Figures 3A and 3C), as well as when the C3H/HeJ strain was reconstituted with WT BM (Figure 3B). However, the expression of FcγRII and FcγRIII was unaltered in either approach (data not shown).

Because the ICAM-1 and LFA-1 axis (expressed on FDCs and GC B cells, respectively) is pivotal for robust GC responses (Koopman et al., 1991, 1994; Kosco et al., 1992), we speculated that blocking TLR4 function would have a profound effect on GC development. Thus, we explored the consequences of decreased ICAM-1 expression resulting from the neutralization of TLR4 signaling by applying a hybrid agent-based mathematical model of the GC reaction (Figge et al., 2008; Meyer-Hermann et al., 2009). The model (Figure 4) assumes that lower ICAM-1 expression reduces the probability of B cell-FDC interactions, thus altering the frequency of Ag uptake by B cells from FDCs. In these simulations, the initial phase of GC B cell expansion is independent of FDC-ICAM-1 expression (Figure 3D). However, from day 6, when B cells are undergoing affinity-dependent selection on FDC-retained Ag, a dose-dependent relationship is exhibited (Figure 3D). Thus, higher expression of ICAM-1 on FDC is associated with larger GCs.

To validate our theoretical approach, we performed in vivo experiments measuring the number of GC B cells per LN when impairing TLR4 function in FDC. Indeed, the number of GC B cells was reduced, suggesting a dependence of the overall efficiency of the GC reaction on intact TLR4-mediated signaling in FDCs (Figures 3E and 3F). Interfering with TLR4 signaling also compromised the size (Figures 3H and 3J) and number (Figure 3I) of GCs per LN. Hence, although not being able to rule out causal relationships to other factors, the in silico-generated data were able to predict that the number of GC B cells per LN would correlate in vivo with ICAM-1 expression on FDCs (Figure 3G), giving us confidence to further exploit the modeling prior to designing in vivo protocols.

Attenuation of TLR4 Responses on FDCs Alters Both Primary and Secondary Humoral Responses

Figure 5A shows the theoretical kinetic dose-response curve of cumulated output cells per GC as ICAM is varied. With time,

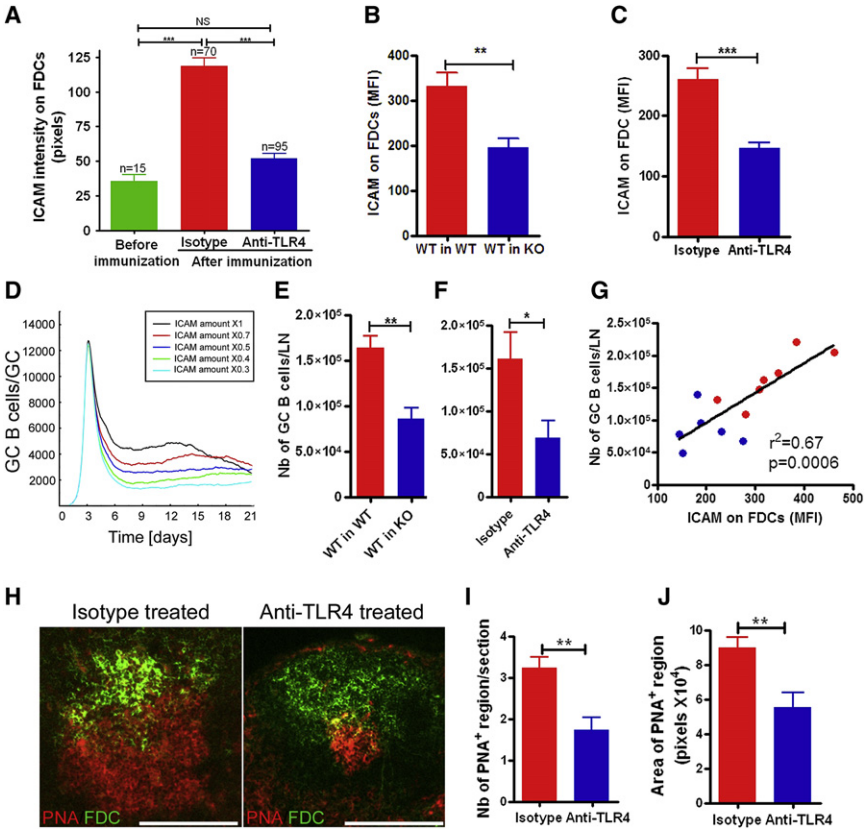

Figure 3. TLR4 Signaling by FDCs Shapes FDC Maturation and the Extent of GC Reactions

(A) ICAM-1 expression is upregulated on FDCs upon maturation and blocked by anti-TLR4 treatment. Balb/c mice treated with anti-TLR4 or isotype control (n = 5/group) were immunized s.c. with OVA plus LPS, and 7 days later sections were prepared from the LNs and labeled with FDC-M2 and anti-ICAM-1. Unimmunized mice were used as control (n = 5). The values are the intensity of expression of the FDC network, analyzed with the AxioVision Rel. 4.6 software. Numbers above the bars correspond to the number of FDC networks analyzed.

(B and C) ICAM-1 expression on FDCs was assayed by flow cytometry with LNs of mice immunized with OVA plus LPS for 10 days. C3H chimeric mice (B) or Balb/c mice treated with anti-TLR4 or isotype control (C) were evaluated (10 mice/group) and the results are representative of two independent experiments.

(D) Time course of simulating the number of GC B cells per GC as a function of FDC-associated ICAM-1 expression.

(E and F) The number of GC B cells was assayed by flow cytometry with the same cells as described in (B) and (C) above.

(G) Linear regression curve obtained from the results displayed in (B), (C), (E), and (F) demonstrating the correlation between the number of GC B cells and amount of ICAM-1 expression on FDCs.

(H–J) Evaluation of LNs obtained from Balb/c mice treated with TLR4 mAb or isotype mAb control 10 days postimmunization. Photomicrographs (H) of representative cryosections labeled with PNA and FDC-M2. Five mice were used per group for which the LNs were entirely cut, immunolabeled, and analyzed to assay the number (I) and the size of the GC (J) with (5E3) or without (isotype control) TLR4 neutralization. The white bar in a photomicrograph represents its relative scale within the figure.

Results represent mean ± SEM.

the model predicts that the number of output cells (e.g., Ag-specific plasma cells) will decrease as a function of lower ICAM expression. Consequently, Ag-specific antibody (Ab) titers and Ig class switch from IgM to IgG isotypes should be lower when TLR4 is lacking. Indeed, a substantial reduction in the anti-OVA primary and secondary IgM (Figure 5B) and secondary IgG responses (Figure 5C) were observed when TLR4 was nonfunctional on FDCs (WT in *Tlr4*$^{-/-}$ BM chimeras compared to WT in WT). Similar results were obtained with anti-TLR4-treated mice for OVA plus LPS or OVA plus alum immunizations (data not shown). The TLR4-dependent effect on IgM titers was obvious at later stages of the response (e.g., after day 6) as predicted by the model, when the output from GCs should have been considerably affected. In contrast, the early phase, when IgM is produced by extrafollicular plasma cells, i.e., a GC-independent pathway (MacLennan et al., 2003), was unaffected by impairing TLR4 function (Figure 5B). Together these mathematical and experimental results infer that TLR4 expression impacts on the production of plasma cells in GCs.

TLR4 Neutralization Abates High-Affinity Ig Responses

Because FDC-B cell contacts influence the selection of clones displaying high affinity for the Ag, we modeled the influence of ICAM-1 expression on FDCs for the generation of high-affinity GC B cells. Together with a decreased output of cells (Figure 5A), the simulations predicted that suboptimal ICAM-1 expression on FDCs would be sufficient to affect affinity maturation leading to an overall decreased number (Figure 5D) but not to a changed fraction (Figure 5E) of high-affinity GC output cells.

To test this prediction, high-affinity Ab titers were measured after a primary immunization and while neutralizing TLR4. These animals displayed weaker total and high-affinity IgG1 responses (Figure 5F). However, in contrast to simulation data, the high-affinity compartment was particularly impacted as reflected by a strongly reduced ratio of high to total anti-NP IgG1 titers by day 21 (Figure 5G). In comparison to IgM, TLR4 neutralization affected high-affinity IgG1 titers preferentially at later time points as shown by the altered ratio of high-affinity IgG to IgM (Figure 5H) during the GC reaction (days 14 and 21 postimmunization; $p < 0.0001$, 2-way ANOVA test). This effect was also seen with total IgG1 versus IgM titers, although the difference was less pronounced (data not shown). These results imply that TLR4 signaling mainly affects GC function (where high-affinity IgG1 develops) rather than extrafollicular site development, where short-lived IgM-secreting plasma cells are produced. In addition, this altered ratio in IgG1/IgM production could reflect a defect in Ig isotype switching, consistent with the function of FDCs in the GC reaction. Finally, in order to evaluate the prolonged impact of TLR4 neutralization on different IgG subtypes, sera from mice receiving a booster immunization were further screened. In these

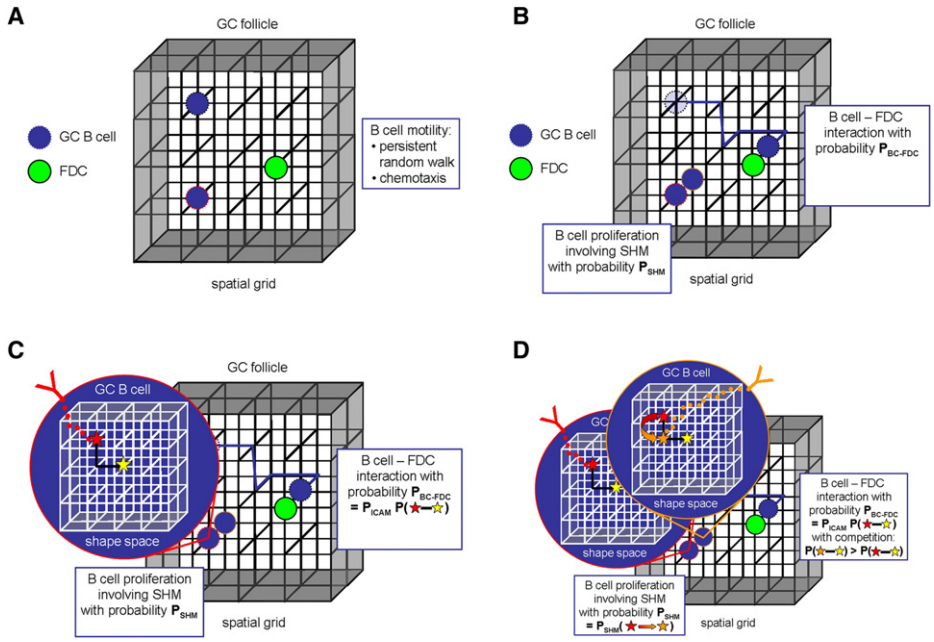

Figure 4. Illustration of the Hybrid Agent-Based Model as Applied in the Computer Simulations of GC Reaction

(A) The B cell follicle in which GCs occur is represented by a three-dimensional spatial grid. B cells (blue) migrate on the spatial grid, performing a persistent random walk or through a chemotactic gradient.

(B) B cells proliferate and undergo SHM with probability P_{SHM}/division. Migrating B cells interact with Ag-presenting FDCs (green) with probability P_{BC-FDC}.

(C) The interaction probability P_{BC-FDC} depends on the distance between the expressed Ab of the B cell (colored star) and the position of the Ag (yellow star) in shape space. The shape space has four dimensions and distances are measured as the shortest path between two points. In addition to the affinity-dependent contribution, P_{BC-FDC} is biased by the ICAM-1 expression on FDCs represented by probability P_{ICAM}. This probability is varied in the simulations to mimic reduced ICAM-1 expression as a consequence of an impairment of TLR4 signaling.

(D) The impact of this impairment on the rate of SHM is taken into account by the probability P_{SHM}. Mutations correspond to moves in the shape space that are performed with probability P_{SHM}/division. The affinity-dependent competition between B cells for survival signals from FDCs is taken into account, since the probability P_{BC-FDC} is a function of the distance between Ab and Ag in shape space.

experiments, the titers for total as well as high-affinity Ag-specific IgG1 (Figures 5I and 5J) as well as IgG2a (Figures S2A and S2B) and IgG2b (Figures S2C and S2D) were substantially impaired. Thus, the generation of high-affinity antibodies was consistently more severely impacted than that of low-affinity antibodies. These results suggest that TLR4 expression on FDCs impacts affinity maturation of Ig responses.

Impairment of TLR4 Function on FDCs Reduces SHM

The model predicted that reduced ICAM-1 expression would not alter the fraction of high-affinity output cells (Figure 5E), yet a decrease was observed through in vivo experimentation, so we explored other potential parameters in silico that might explain this discrepancy between the model and biological experiment. As shown in Figure 6A, in our model the fraction of high-affinity output cells will decrease as a function of mutation frequency rates per cell division (not the absolute number of mutations) (Figure 6A, solid black and gray lines). Combining reduced SHM with reduced ICAM-1 expression has only a weak additive effect on the fraction of high-affinity output cells (Figure 6A, dashed-dotted black and gray lines). Also, the number of GC B cells per GC remains unaltered by reduced SHM frequencies (Figure 6B; compare the two solid lines or the two dashed-dotted lines for ICAM-1 reduced by a factor of 0.4). In order to determine the robustness of phenotypes other than the fraction of high-affinity output cells, we further reduced the SHM rate and found that other phenotypes were modified only when the SHM rate was reduced to 10% of control (Figure 6B, dotted line). Thus, in a reasonable range, reduced SHM rates selectively impact on the fraction of high-affinity output cells produced in GCs. Note that if the mutation rate is changed via the B cell proliferation rate, the in silico-observed impact extends to other phenotypes. In conclusion, the simulation results would agree with the experiments (including the observed reduction in the fraction of high-affinity cells) when assuming that the suppressed TLR4 signaling would concurrently inhibit ICAM-1 and SHM in vivo.

Experiments were then designed to test these in silico predictions in vivo. The rearranged *V_H186.2* gene, which characterizes the heavy chain of the anti-NP Ab, was specifically amplified with cDNA from GC B cells isolated from immunized C3H chimeric mice as well as naive B cells isolated from nonimmunized chimeric mice (used as the background mutation control). As shown in Figure 6C, the rate of nucleotide (Nt) mutations in the CDR regions of the *V_H186.2* gene was reduced by 50% in the GC B cells obtained from the chimera deficient for TLR4 function on their FDCs (6×10^{-2} versus 14×10^{-2} for mice sufficient for TLR4) confirming the in silico prediction. Whereas the pattern of Nt substitutions did not change between the two groups (Figure 6D), AID hotspots were less susceptible to mutations (Figure 6E), suggesting an alteration of AID activity in GC B cells

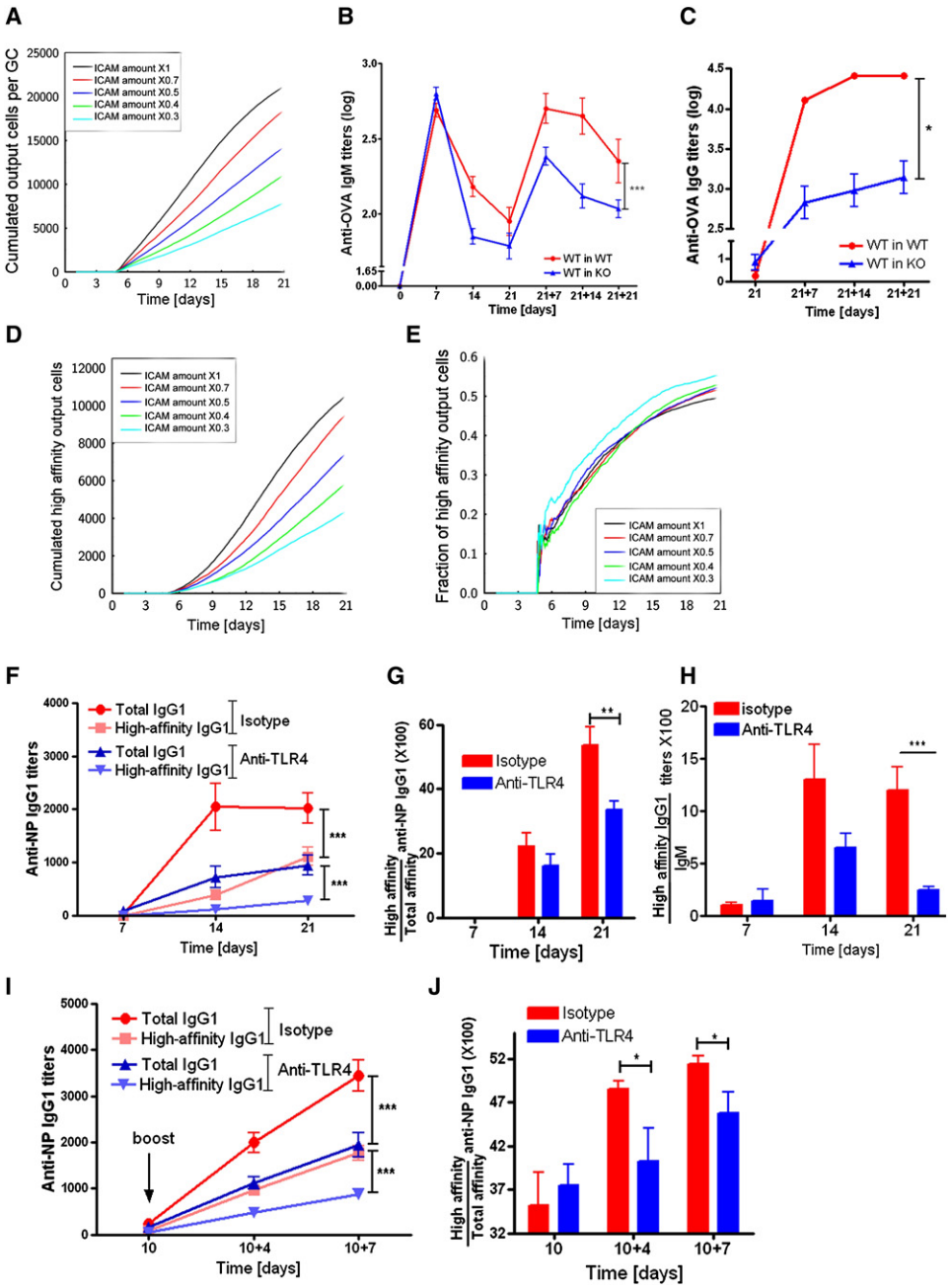

Figure 5. TLR4 Signaling by FDCs Modifies the Humoral Response and High-Affinity Ig Production

(A) Time course of simulating the number of output cells (plasma cells) generated per GC as a function of varying FDC-associated ICAM-1.

(B and C) Reconstituted C3H chimeric mice (n = 15/group) were immunized with OVA plus LPS and boosted with OVA at day 21. Sera were collected weekly and Ag-specific IgM (B) and IgG (C) titers were established by ELISA. The results are representative of three independent experiments.

(D and E) Time course of simulating the number (D) and fraction (E) of high-affinity plasma cells leaving the GC as a function of varying FDC-associated ICAM-1.

(F–H) Balb/c mice treated with the anti-TLR4 or isotype control (n = 10/group) were immunized with NP-OVA plus LPS, sera were collected weekly, and the NP-specific IgG1 (F) titers were established by ELISA. High-affinity NP-specific Ig to the total amount of Ig (G) or the high-affinity NP-specific IgG1 to IgM (H) ratios plotted over the time course for titers incurred by the primary immunization. Data are representative of three independent experiments.

(I and J) Balb/c mice (n = 10/group) were immunized with NP-OVA plus LPS, boosted after 10 days with NP-OVA in PBS, and treated with the anti-TLR4 or isotype control. Sera were collected, NP-specific IgG1 (I) titers were established by ELISA, and the ratio of high-affinity NP-specific IgG1 to the total IgG1 is plotted over the time course after the primary (10 days) and secondary (10+4; 10+7 days) immunization (J).

Results represent mean ± SEM. See also Figure S2.

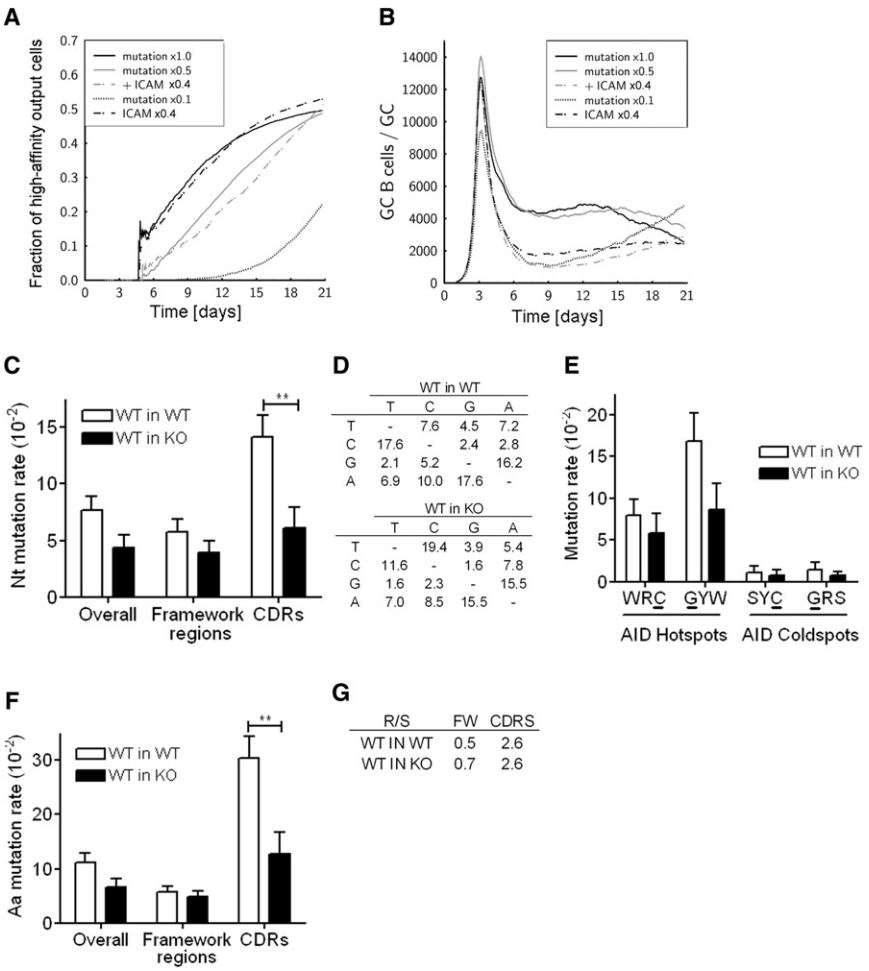

Figure 6. TLR4 Signaling by FDCs Influences Rates of SHM during the GC Reaction

(A and B) Time course of simulating the fraction of high-affinity output cells (A) and the number of GC B cells generated per GC (B) as function of varying the rate of mutation with (+) and without concomitant alteration in ICAM-1 expression on FDCs.

(C–G) LNs of C3H chimeric mice, immunized with NP-OVA plus LPS and boosted with NP-OVA, were obtained 10 days after second immunization (n = 8/group). 10^6 GC B cells were sorted by flow cytometry. Naive $CD19^+IgD^+$ B cells from LNs of nonimmunized littermate chimeras were sorted to serve as the reference controls. cDNA from each group was amplified by nested PCR to obtain the $V_H186.2$ gene and 40 individual clones were sequenced.

(C and F) Mutation rates in nucleotides (Nts; C) and amino acids (Aa; F) in the overall, CDR, and Ig framework regions. 2-way ANOVA tests performed between the "WT in WT" and the "WT in KO" groups indicated statistical differences in the mutation rate ($p = 0.002$ for the Nts and $p < 0.0001$ for the Aa), KO defining the $Tlr4^{-/-}$ genotype.

(D) Percentage of Nt substitutions within the $V_H186.2$ gene.

(E) Mutation rates in AID hotspots and coldspots of the overall $V_H186.2$ gene. W = A or T; R = A or G; Y = C or T; S = G or C. 2-way ANOVA tests indicated statistical differences between the "WT in WT" and the "WT in KO" groups for the hotspots ($p < 0.0001$) but not for the coldspots.

(G) Ratios of replacement (R) versus silent (S) mutations in the framework regions (FW) and CDRs.

Results represent mean ± SEM.

of animals with defective TLR4 on their FDCs. These differences in Nt sequences were translated into changes in amino acids (Aa) (Figure 6F) without affecting the ratio of replacement/silent mutations (Figure 6G).

Interestingly, when TLR4 was defective on FDCs, 15% of the clones shared identical Nt sequences (3/20), whereas 32% were found to be identical in mice sufficient for TLR4 (6/19). This phenomenon was also confirmed when translating Nt codes into Aa sequences (15% of redundancy for the TLR4-deficient mice versus 37% for the TLR4-sufficient mice). This result reinforces the importance of TLR4 function on FDCs for affinity maturation. In summary, these experiments confirmed the in silico prediction, suggesting that a lack of TLR4 signaling on FDCs negatively impacts the efficiency of SHM in the GC, thus explaining the strongly reduced ratio of high-affinity Ab titers found in vivo (Figures 5F–5J).

Lack of TLR4 Function in FDCs Alters the Gene Expression Profile of FDCs

In order to further understand the effects of impairing TLR4 signaling by FDCs, the expression of genes involved in FDC network maintenance (*LTβR*), cell adhesion (*ICAM-1*, *VCAM-1*, *CD44*), GC formation (*CCL19*, *CCL21*, *CXCL12*, *CXCL13*, and *RGS-1*), isotype switching (*IL-6*), and humoral responses (*IL-10* and *IL-15*) were investigated. Purified FDCs from immune mice treated with the anti-TLR4 displayed lower mRNA expression for ICAM-1, but not for other adhesion molecules tested, i.e., CD44 and VCAM-1 (Figure 7A). LTβR mRNA expression by FDCs was also decreased (Figure 7B), as well as mRNA expression of the cytokines IL-1β, IL-6, IL-10, and IL-15 (Figure 7C) and the chemokines CCL19, CCL21, and CXCL12 (Figure 7D).

Next, the effect of impairing FDC-associated TLR4 signaling on gene expression in GC B cells was investigated with the previously described chimeric mice. None of the apoptosis-related genes tested were altered (Figure 7E). This result was predicted by the in silico model (Figures S3A and S3B) and confirmed by Annexin V labeling on GC B cells from mice treated with the TLR4 mAb. mRNA encoding the proliferation marker Ki67 was downregulated in the GC B cells from mice with nonfunctional TLR4 on FDCs (Figure 7F) as well as the mRNA for AID, albeit only by 20% (Figure 7F).

Finally, the mRNA for RGS-1, a protein involved in desensitization to prolonged chemokine exposure, was also downregulated (Figure 7F). Because investigating the effect of this parameter, i.e., an alteration in chemokine receptor desensitization in vivo, would require currently unavailable tools, we decided to model

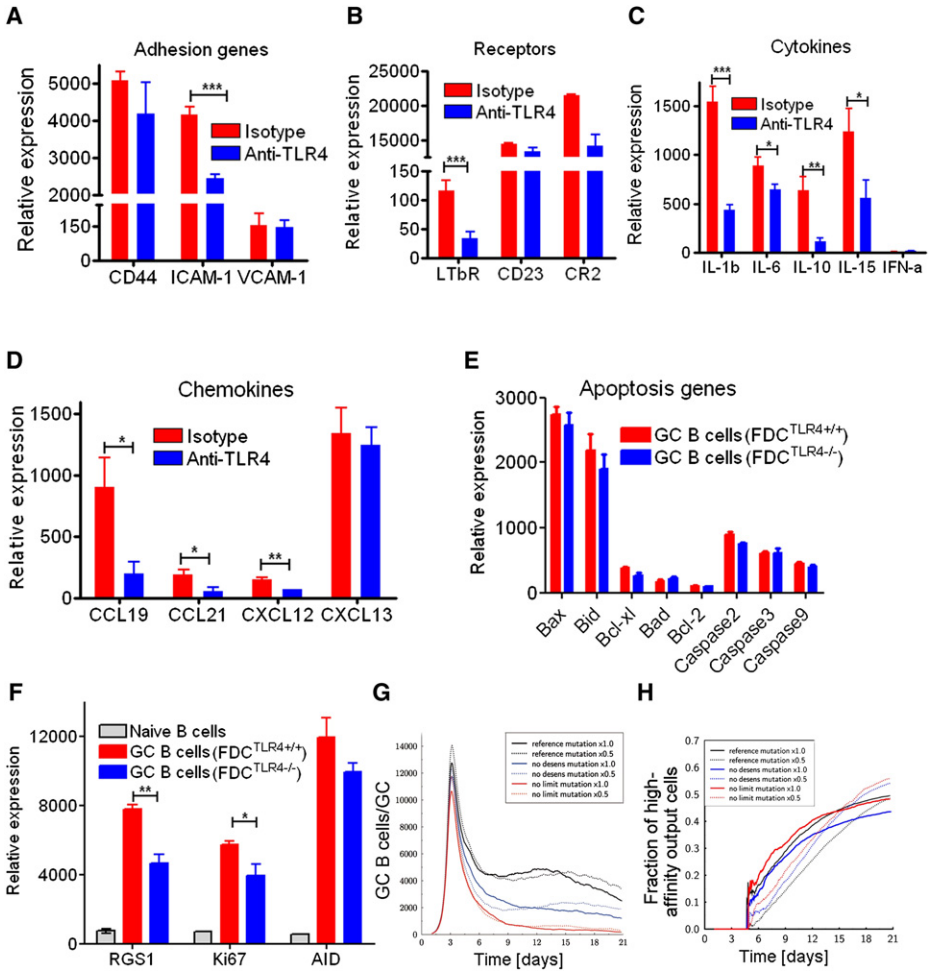

Figure 7. TLR4 Signaling by FDCs Impacts the Expression of Genes Critical for GC Reactions

(A–D) LNs from Balb/c mice treated with the anti-TLR4 or isotype control (n = 20 LNs/group) were obtained 7 days after immunization with OVA plus LPS. From 10^5 FDCs isolated by flow cytometry, RNA extraction and cDNA synthesis were performed. Q-PCRs were done twice in quadruplicate for genes involved in GC function.

(E and F) LNs of C3H chimeric mice (WT in WT mice are defined as FDC *Tlr4*$^{+/+}$; WT in KO as FDC *Tlr4*$^{-/-}$) were obtained 10 days after immunization with NP-OVA plus LPS (n = 8 LNs/group). From 10^6 GC B cells isolated by flow cytometry, RNA extraction and cDNA synthesis were performed. Q-PCRs were done twice in quadruplicate for genes involved in GC function.

(G and H) Time course simulating the number of GC B cells (G) and the fraction of high-affinity output cells (H) with (dotted lines) or without (full lines) reduced SHM rate for different desensitization models. In the *reference* simulation (black lines), B cells, after upregulation of the chemokine receptor, desensitize in a chemokine concentration-dependent way and after 6 hr at the latest. Then, the concentration-dependent desensitization is switched off (*no desens,* blue lines) or desensitization is fully blocked (*no limit,* red lines).

Results represent mean ± SEM. See also Figure S3.

this in silico (Figures 7G and 7H). The effect associated with the downregulation of RGS-1 expression in GC B cells was modeled with three considerations (Figures 7G and 7H), that is, desensitization (*reference*), desensitization only after 6 hr (*no desens*), and a total absence of chemokine receptor desensitization (*no limit*). Comparing the results demonstrated that lacking some sort of a chemokine receptor desensitization process would lead to a reduction in the number of GC B cells (Figure 7G) but would not have a substantial effect on the fraction of high-affinity output cells (Figure 7H). The effect of suppressed desensitization, thus, correlates with that observed for ICAM-1 inhibition. Taken together, these results suggest that RGS-1 is candidate for a critical protein regulated by FDC-associated TLR4 signaling.

DISCUSSION

DCs and FDCs are central to immune responses: both are implicated in exposing immunogenic epitopes of pathogens to T and B cells via peptides associated with major histocompatibility complexes (MHC) or in the form of whole Ag as immune complexes (ICs) on complement and Fc receptors. The maturation of both cell types has been reported to be mediated via TLR4 triggering (Lee and Iwasaki, 2007; El Shikh et al., 2007). The direct consequences of altering DC maturation are well described and lead to a defect in T cell adaptive immune responses (Banchereau and Steinman, 1998). In the present study, we provide evidence that FDCs express and upregulate

TLR4 in situ during germinal center reactions, confirm that their maturation is driven by TLR4, and associate the role of FDC-expressed TLR4 with quantitative and qualitative effects of GC B cell responses.

Demonstrating that TLR4 expression during the GC reaction was restricted and overlapping with the FDC-specific Ab, FDC-M2, in a immunohistochemical kinetic study conducted on tissue sections is a striking result. The highly limited degree of colabeling within the microenvironment on the well-defined FDC network demonstrates a role of TLR4 signaling by radioresistant FDCs, at least during the phases of the GC reaction. However, although we acknowledge that these data are consistent with FDCs mediating these effects, it is not possible to exclude the contribution of additional radioresistant cell types that express TLR4 at levels that are undetectable by fluorescence microscopy and may be biologically important. Our results aim to resolve the controversy occurring in the literature (Pasare and Medzhitov, 2005; Nemazee et al., 2006; Meyer-Bahlburg et al., 2007) and exclude that the humoral response is not influenced by TLR4 signaling by FDCs. Interestingly, a very recent paper has described the influence of TLR4 signaling in B cells (Hwang et al., 2009). In that study, the authors reported enhanced migration and proliferative proprieties of ex vivo LPS *pretreated* B cells although without alteration of the secondary IgG response. We did not observe a restricted access to the GC when inhibiting TLR4 signaling by FDCs, but rather a functional impairment of GC function, so we speculate that the role of TLR4 on B cells and FDCs may be totally different and affect different aspects of the timing for TLR4 signaling on each population: TLR4 signaling on B cells would influence the migration of B cells into the microenvironment, impacting on eventual proliferation, whereas TLR4 signaling on the FDCs alters molecules important to generate high-affinity, isotype-switched, Ag-specific Abs.

Interestingly, as observed with DCs, a direct effect of impairing TLR4 function on FDCs is also an inhibition of their maturation, observed by a decrease in ICAM-1 expression, the adhesion molecule involved in their interaction with B cells via LFA-1 (Koopman et al., 1991). We speculated that such a defect in ICAM-1 expression would alter the GC reaction and addressed this question by modeling the consequences of a reduced binding probability of centrocytes to FDCs in silico. We found in vivo and in silico a reduction in GC B cells, associated with a decreased humoral response and high-affinity B cell number. Our simulations suggested that SHM should also be impaired in TLR4-deficient mice, which was confirmed in vivo. Furthermore, the expression of LTβR in TLR4-deficient FDCs was changed. The LTα-LTβR axis is required for GC formation (Matsumoto et al., 1996b), SHM, and affinity maturation (Matsumoto et al., 1996a). In accordance, our results lead us to think that the LT-α-LTβR axis may be affected by impaired TLR4 triggering and that alteration of LTβR expression on FDCs, probably secondary to loss of FDC maturation, would accelerate FDC network decay, simultaneously affecting several parameters of FDC-mediated GC function.

One other consequence of interfering with FDC maturation is the impairment of their cytokine production. Indeed, we observed an alteration of the expression of IL-1β (involved in GC B cell proliferation) and IL-10 (which drives B cell differentiation toward plasmablasts). The expression of two other cytokines produced by activated FDCs (Husson et al., 2000), namely IL-6 (involved in isotype switch [Van et al., 1994]) and IL-15 (which helps GC B cell proliferation [Park et al., 2004]), was also reduced. Concurrently with the inhibition of expression of these cytokines by FDCs, the downregulation of proliferation markers Ki67 and AID (the enzyme involved in SHM) was observed in the GC B cells, highlighting the possible role of these cytokines in affecting these parameters. It is, however, hard to imagine that this small inhibition of AID expression could be responsible for the observed 50% reduction of SHM. It is, therefore, likely that other mechanisms may be involved, such as an alteration in AID activity, suggested by a decreased number of mutations in AID hotspots as well as a decrease in the expression of essential partners of AID, e.g., the protein kinase A alpha regulatory subunit (PKAr1α) (Basu et al., 2005), or other molecules involved in SHM, like uracyl-DNA glycosylase (UNG) (Di Noia and Neuberger, 2002) or Rev1 (Nelson et al., 1996).

Impairment of TLR4 signaling in FDCs did not inhibit the expression of CXCL13, the major FDC-secreted chemokine, whose regulation was independent of ICAM-1, TLR4, and LT-α-LTβR. Even though CCL19 and CCL21 have not yet been reported to be expressed by FDCs, the mRNA of these chemokines appear to be decreased when TLR4 signaling was blocked or inhibited. This result may be related to the purity of the FDC preparation (i.e., 90%). In parallel, we observed that the mRNA expression of RGS-1, a molecule involved in chemokine receptor desensitization, was reduced by almost 50% in GC B cells from chimeric mice lacking TLR4 function on FDCs. However, in silico simulations indicate that only stronger disruptions of chemokine receptor desensitization will impact on the organization of B cells and affinity maturation. Thus, FDC TLR4 signaling does not appear to impact GC B cell migration to a substantial extent.

It is tempting to speculate as to how these alterations in gene expression, resulting from the impairment of FDC TLR4 function, contribute to the alteration of GC function. For instance, a decrease in IL-10 would drive a shift from generating plasma cells toward memory B cells. Thus, IL-10 would impact on the Ig titers but leave the number of GC B cells mainly unaffected. Similarly, according to the simulations, ICAM-1 expression is not correlated with the fraction of high-affinity cells but induces an unspecific reduction of the GC B cell population whereas a 50% reduction of the SHM rate does not affect the number of GC B cells but specifically reduces the fraction of high-affinity cells. However, the combined effect of ICAM-1 and SHM adds up to the observed experimental result. Because of the inherently interwoven actors, it is difficult to disentangle their individual role and mathematical simulations help in that respect.

On a more general note, our results illustrate that experiments in biology can take advantage of mathematical modeling. Even though mathematics cannot claim that a mechanism is necessary, the modeling allows us to state that it is sufficient to identify specific phenotypes and by this to help design focused and conclusive research. Not only is this resource friendly and rapid but it is also ethically appealing in that the number of in vivo experiments could be significantly decreased by predicting which parameters were most likely to be relevant. Thus, innovative computer simulations allow a systematic analysis of complex systems and the deduction of causal relationships between manipulated parameters and observable effects.

A potential scenario to explain our observations is to suggest that as apoptotic bodies arise during a GC reaction, they trigger activation of FDCs through TLR4. As a consequence, cytokines would be produced, affecting various downstream events culminating in the production of high-affinity Ig. IL-1β and IL-15 would aid in GC B cell proliferation, IL-10 would aid in the generation of plasmablasts, and IL-6 would enhance Ig isotype switch and SHM. Our results therefore delineate a concept in which endogenous ligands, such as the remnants of dying cells providing OxPl, as well as heat shock proteins (Wheeler et al., 2009), and even HMGB-1 would serve an important function for the overall efficiency of the GC reaction by activating FDCs via TLR4.

The body's capacity to successfully battle pathogens depends on raising Abs that have a strong binding capacity and appropriate Ig backbone. Generating these Abs occurs spatially and temporally in germinal center reactions. TLR4 senses elements of pathogens and inflammation igniting the immune system into action. The work presented here shows that TLR4 activation will induce the onset of germinal center formation and set up the microenvironment to induce B cells to undergo SHM and Ig class switch. The TLR4 signaling occurs not in the germinal center B cell, but rather in the FDC. TLR4 signaling by FDCs shapes their maturation and creates molecules necessary for germinal center output. Iterative cycles of modeling these components facilitated the investigative research by directing experiments along certain hypotheses. Creating pathogen-specific Abs are central to vaccine strategies and uncontrolled, exaggerated Ab responses are a hallmark of many autoimmune diseases, thus demonstrating that TLR4 signaling in FDCs sets the stage for new therapeutic strategies that will apply across many fields of medicine.

EXPERIMENTAL PROCEDURES

Animals

Experiments were performed in accordance with Swiss experimental animal regulations, with 8-week-old Balb/c (Janvier Laboratories, Le Genest-St-Isle, France), C3H/HeJ (Jackson Laboratory, Bar Harbor, ME), or C3H/HeN (Charles River Laboratory, L'Arbresle, France) mice.

Irradiation and Chimera Generation

C3H/HeJ or C3H/HeN mice were lethally irradiated (800 rad), checked for absence of leukocytes in blood 24 hr later, and intravenously (i.v.) transplanted with 5×10^6 BM cells from C3H/HeJ or C3H/HeN donor mice. Successful grafting was determined by flow cytometry of peripheral blood 4 weeks after transplantation. Immunizations were performed 6–8 weeks after BM transplant.

Immunization and Treatment

All immunizations were performed subcutaneously behind the neck. For the primary immunization, a mixture of 100 μg of OVA (Sigma, Saint-Louis, MO) and 250 μg of LPS (*E. coli*, strain 0111:B4, Sigma) was injected. Three weeks later, mice received a booster immunization with 25 μg of OVA in PBS. To assay low- and high-affinity Ab production, Balb/c mice were immunized with a mixture of 20 μg of NP-OVA (Biosearch Technologies; Novato, CA) and 150 μg of LPS or primed and boosted at day 10 with 5 μg of NP-OVA in PBS. Balb/c mice were administered daily intraperitoneal (i.p.) doses of 100 μg of the blocking, nondepleting anti-mouse TLR4 mAb, 5E3, generated in our laboratory (Daubeuf et al., 2007) or with an isotype control starting 3 days after the primary immunization. To measure the SHM rate, chimeric C3H mice were immunized with a mixture of 20 μg of NP-OVA and 150 μg of LPS, then boosted after 4 weeks with 5 μg of NP-OVA in PBS.

ELISA

96-well plates (NUNC, Rochester, NY) were coated overnight at 4°C with NP7-BSA or NP23-BSA (Biosearch Technologies) (10 μg/ml) for the affinity ELISAs or with OVA (2 μg/ml) for regular ELISAs. The whole protocol is detailed in the Supplemental Experimental Procedures.

Histology

LN samples were prepared, sectioned, and immunostained as previously described (Furtado et al., 2007) and as detailed in the Supplemental Experimental Procedures.

Flow Cytometry

Cells from LNs were obtained by collagenase/DNase digestion, followed by 1 hr incubation at 37°C to remove adherent macrophages. Directly conjugated Abs were incubated at 4°C in FACS buffer (PBS/BSA 1%) for 1 hr and indirect labeling was followed by a 30 min incubation time via secondary conjugated Abs. To exclude dead cells, propidium iodine (PI) was added before the analysis performed on the FACSCalibur flow cytometer (BD).

Sorting by Flow Cytometry

After enzyme digestion and adherence step procedure, as detailed above to isolate cells from immunized LNs, FDCs or GC B cells were further purified by cell sorting. The isolated cells were colabeled with a cocktail for (CD21/35) and FDC-M2 to sort the FDC population, or PNA, CD19, and Fas to sort the GC B cells. Sorting was performed with the FACS Vantage (BD) and cells were collected in RNAlater (Ambion, Austin, TX). Cell sorting containing a purity higher than 90% were kept for RNA extraction.

RNA Extraction and cDNA Generation

RNA from FDCs was extracted with the RNAqueous-Micro Kit (Ambion) according to the manufacturer's instructions. 500 ng of RNA was reverse transcribed with the High Capacity cDNA Reverse Transcription Kit (Applied Biosystems, Foster City, CA).

Quantitative PCR

Q-PCR was conducted as previously described (Furtado et al., 2007) and as detailed in the Supplemental Experimental Procedures.

Somatic Hypermutation

Because the anti-NP response is known to predominantly use the $V_H186.2$ gene (Jacob et al., 1991; Rajewsky et al., 1987), this heavy V gene usage was analyzed to assess SHM. GC B cells were sorted from LNs of the C3H chimerae, 10 days after the second immunization. In parallel, naive $CD19^+/IgD^+$ B cells from LNs of nonimmunized littermate chimeras were sorted to serve as references, because the germline sequence of the $V_H186.2$ gene in C3H strain is unknown. Cell sorting, RNA isolation, cDNA synthesis, amplification of the $V_H186.2$ gene, and cloning of the PCR products are performed according to the procedure detailed in the Supplemental Experimental Procedures.

Mathematical Modeling

Computer simulations were performed covering the full time course of a GC reaction at the level of individual cells that migrate and interact in the three-dimensional spatially resolved follicle. The used simulation is a hybrid agent-based model that was developed and validated since 2001 (Meyer-Hermann et al., 2001) and has proven to have predictive power in various circumstances (Meyer-Hermann et al., 2009) and detailed in the Supplemental Experimental Procedures.

Statistics

To evaluate statistical differences, the unpaired two-tailed Student's t or two-way Anova tests were applied as indicated. p values less than 0.05 were considered statistically significant and the following designation used: $*p < 0.05$; $**p < 0.01$; and $***p < 0.001$.

SUPPLEMENTAL INFORMATION

Supplemental Information includes Supplemental Experimental Procedures and four figures and can be found with this article online at doi:10.1016/j.immuni.2010.07.005.

ACKNOWLEDGMENTS

The authors want to thank J.L. Witztum for providing us with the EO6 Ab and B. Huard for technical assistance. This research was supported by the EU within the NEST project MAMOCELL. M.M.-H. is supported by ALTANA AG. V.B., G.E., and M.H.K.-V. are employees and shareholders of NovImmune SA.

A.G. and M.H.K.-V. planned and analyzed the in vivo experiments and prepared the manuscript; A.G. performed the in vivo experiments; M.M.-H. performed the in silico experiments; M.C. generated the SHM data; V.B. generated flow cytometry data; M.M.-H. and M.T.F. planned and analyzed the in silico simulations and helped draft the manuscript; and M.G., K.-M.T., and G.E. participated in designing experiments and reviewed the manuscript.

Received: November 27, 2008
Revised: April 8, 2010
Accepted: July 5, 2010
Published online: July 22, 2010

REFERENCES

Akira, S., Takeda, K., and Kaisho, T. (2001). Toll-like receptors: Critical proteins linking innate and acquired immunity. Nat. Immunol. *2*, 675–680.

Akira, S., Uematsu, S., and Takeuchi, O. (2006). Pathogen recognition and innate immunity. Cell *124*, 783–801.

Aydar, Y., Sukumar, S., Szakal, A.K., and Tew, J.G. (2005). The influence of immune complex-bearing follicular dendritic cells on the IgM response, Ig class switching, and production of high affinity IgG. J. Immunol. *174*, 5358–5366.

Banchereau, J., and Steinman, R.M. (1998). Dendritic cells and the control of immunity. Nature *392*, 245–252.

Banerjee, A., and Gerondakis, S. (2007). Coordinating TLR-activated signaling pathways in cells of the immune system. Immunol. Cell Biol. *85*, 420–424.

Basu, U., Chaudhuri, J., Alpert, C., Dutt, S., Ranganath, S., Li, G., Schrum, J.P., Manis, J.P., and Alt, F.W. (2005). The AID antibody diversification enzyme is regulated by protein kinase A phosphorylation. Nature *438*, 508–511.

Chang, M.K., Bergmark, C., Laurila, A., Horkko, S., Han, K.H., Friedman, P., Dennis, E.A., and Witztum, J.L. (1999). Monoclonal antibodies against oxidized low-density lipoprotein bind to apoptotic cells and inhibit their phagocytosis by elicited macrophages: Evidence that oxidation-specific epitopes mediate macrophage recognition. Proc. Natl. Acad. Sci. USA *96*, 6353–6358.

Daubeuf, B., Mathison, J., Spiller, S., Hugues, S., Herren, S., Ferlin, W., Kosco-Vilbois, M., Wagner, H., Kirschning, C.J., Ulevitch, R., and Elson, G. (2007). TLR4/MD-2 monoclonal antibody therapy affords protection in experimental models of septic shock. J. Immunol. *179*, 6107–6114.

Di Noia, J., and Neuberger, M.S. (2002). Altering the pathway of immunoglobulin hypermutation by inhibiting uracil-DNA glycosylase. Nature *419*, 43–48.

El Shikh, M.E., El Sayed, R.M., Wu, Y., Szakal, A.K., and Tew, J.G. (2007). TLR4 on follicular dendritic cells: an activation pathway that promotes accessory activity. J. Immunol. *179*, 4444–4450.

Figge, M.T., Garin, A., Gunzer, M., Kosco-Vilbois, M., Toellner, K.M., and Meyer-Hermann, M. (2008). Deriving a germinal center lymphocyte migration model from two-photon data. J. Exp. Med. *205*, 3019–3029.

Furtado, G.C., Marinkovic, T., Martin, A.P., Garin, A., Hoch, B., Hubner, W., Chen, B.K., Genden, E., Skobe, M., and Lira, S.A. (2007). Lymphotoxin beta receptor signaling is required for inflammatory lymphangiogenesis in the thyroid. Proc. Natl. Acad. Sci. USA *104*, 5026–5031.

Gribar, S.C., Anand, R.J., Sodhi, C.P., and Hackam, D.J. (2008). The role of epithelial Toll-like receptor signaling in the pathogenesis of intestinal inflammation. J. Leukoc. Biol. *83*, 493–498.

Humphrey, J.H., Grennan, D., and Sundaram, V. (1984). The origin of follicular dendritic cells in the mouse and the mechanism of trapping of immune complexes on them. Eur. J. Immunol. *14*, 859–864.

Husson, H., Lugli, S.M., Ghia, P., Cardoso, A., Roth, A., Brohmi, K., Carideo, E.G., Choi, Y.S., Browning, J., and Freedman, A.S. (2000). Functional effects of TNF and lymphotoxin alpha1beta2 on FDC-like cells. Cell. Immunol. *203*, 134–143.

Hwang, I.Y., Park, C., Harrison, K., and Kehrl, J.H. (2009). TLR4 signaling augments B lymphocyte migration and overcomes the restriction that limits access to germinal center dark zones. J. Exp. Med. *206*, 2641–2657.

Imai, Y., Kuba, K., Neely, G.G., Yaghubian-Malhami, R., Perkmann, T., van Loo, G., Ermolaeva, M., Veldhuizen, R., Leung, Y.H., Wang, H., et al. (2008). Identification of oxidative stress and Toll-like receptor 4 signaling as a key pathway of acute lung injury. Cell *133*, 235–249.

Iwamura, C., and Nakayama, T. (2008). Toll-like receptors in the respiratory system: Their roles in inflammation. Curr. Allergy Asthma Rep. *8*, 7–13.

Jacob, J., Kelsoe, G., Rajewsky, K., and Weiss, U. (1991). Intraclonal generation of antibody mutants in germinal centres. Nature *354*, 389–392.

Koopman, G., Parmentier, H.K., Schuurman, H.J., Newman, W., Meijer, C.J., and Pals, S.T. (1991). Adhesion of human B cells to follicular dendritic cells involves both the lymphocyte function-associated antigen 1/intercellular adhesion molecule 1 and very late antigen 4/vascular cell adhesion molecule 1 pathways. J. Exp. Med. *173*, 1297–1304.

Koopman, G., Keehnen, R.M., Lindhout, E., Newman, W., Shimizu, Y., van Seventer, G.A., de Groot, C., and Pals, S.T. (1994). Adhesion through the LFA-1 (CD11a/CD18)-ICAM-1 (CD54) and the VLA-4 (CD49d)-VCAM-1 (CD106) pathways prevents apoptosis of germinal center B cells. J. Immunol. *152*, 3760–3767.

Kosco, M.H., Pflugfelder, E., and Gray, D. (1992). Follicular dendritic cell-dependent adhesion and proliferation of B cells in vitro. J. Immunol. *148*, 2331–2339.

Lee, H.K., and Iwasaki, A. (2007). Innate control of adaptive immunity: Dendritic cells and beyond. Semin. Immunol. *19*, 48–55.

Lindhout, E., Mevissen, M.L., Kwekkeboom, J., Tager, J.M., and de Groot, C. (1993). Direct evidence that human follicular dendritic cells (FDC) rescue germinal centre B cells from death by apoptosis. Clin. Exp. Immunol. *91*, 330–336.

MacLennan, I.C., Toellner, K.M., Cunningham, A.F., Serre, K., Sze, D.M., Zuniga, E., Cook, M.C., and Vinuesa, C.G. (2003). Extrafollicular antibody responses. Immunol. Rev. *194*, 8–18.

Marshak-Rothstein, A. (2006). Toll-like receptors in systemic autoimmune disease. Nat. Rev. Immunol. *6*, 823–835.

Matsumoto, M., Lo, S.F., Carruthers, C.J., Min, J., Mariathasan, S., Huang, G., Plas, D.R., Martin, S.M., Geha, R.S., Nahm, M.H., and Chaplin, D.D. (1996a). Affinity maturation without germinal centres in lymphotoxin-alpha-deficient mice. Nature *382*, 462–466.

Matsumoto, M., Mariathasan, S., Nahm, M.H., Baranyay, F., Peschon, J.J., and Chaplin, D.D. (1996b). Role of lymphotoxin and the type I TNF receptor in the formation of germinal centers. Science *271*, 1289–1291.

Meyer-Bahlburg, A., Khim, S., and Rawlings, D.J. (2007). B cell intrinsic TLR signals amplify but are not required for humoral immunity. J. Exp. Med. *204*, 3095–3101.

Meyer-Hermann, M., Deutsch, A., and Or-Guil, M. (2001). Recycling probability and dynamical properties of germinal center reactions. J. Theor. Biol. *210*, 265–285.

Meyer-Hermann, M., Figge, M.T., and Toellner, K.M. (2009). Germinal centres seen through the mathematical eye: B-cell models on the catwalk. Trends Immunol. *30*, 157–164.

Miller, Y.I., Chang, M.K., Binder, C.J., Shaw, P.X., and Witztum, J.L. (2003). Oxidized low density lipoprotein and innate immune receptors. Curr. Opin. Lipidol. *14*, 437–445.

Nelson, J.R., Lawrence, C.W., and Hinkle, D.C. (1996). Deoxycytidyl transferase activity of yeast REV1 protein. Nature *382*, 729–731.

Nemazee, D., Gavin, A., Hoebe, K., and Beutler, B. (2006). Immunology: Toll-like receptors and antibody responses. Nature *441*, E4.

Park, C.S., Yoon, S.O., Armitage, R.J., and Choi, Y.S. (2004). Follicular dendritic cells produce IL-15 that enhances germinal center B cell proliferation in membrane-bound form. J. Immunol. *173*, 6676–6683.

Pasare, C., and Medzhitov, R. (2005). Control of B-cell responses by Toll-like receptors. Nature *438*, 364–368.

Phipps, R.P., Mandel, T.E., and Tew, J.G. (1981). Effect of immunosuppressive agents on antigen retained in lymphoid follicles and collagenous tissue of immune mice. Cell. Immunol. *57*, 505–516.

Poltorak, A., He, X., Smirnova, I., Liu, M.Y., Van, H.C., Du, X., Birdwell, D., Alejos, E., Silva, M., Galanos, C., et al. (1998). Defective LPS signaling in C3H/HeJ and C57BL/10ScCr mice: Mutations in Tlr4 gene. Science *282*, 2085–2088.

Rajewsky, K., Forster, I., and Cumano, A. (1987). Evolutionary and somatic selection of the antibody repertoire in the mouse. Science *238*, 1088–1094.

Van, O.R., Vredendaal, A.E., and Savelkoul, H.F. (1994). Suppression of polyclonal and antigen-specific murine IgG1 but not IgE responses by neutralizing interleukin-6 in vivo. Eur. J. Immunol. *24*, 1396–1403.

Wheeler, D.S., Chase, M.A., Senft, A.P., Poynter, S.E., Wong, H.R., and Page, K. (2009). Extracellular Hsp72, an endogenous DAMP, is released by virally infected airway epithelial cells and activates neutrophils via Toll-like receptor (TLR)-4. Respir. Res. *10*, 31.

Wu, Y., Sukumar, S., El Shikh, M.E., Best, A.M., Szakal, A.K., and Tew, J.G. (2008). Immune complex-bearing follicular dendritic cells deliver a late antigenic signal that promotes somatic hypermutation. J. Immunol. *180*, 281–290.